Journal

Geophysical Research Letters, 52(4)

ISSN

0094-8276

Authors

Carroll, Rosemary WH
Manning, Andrew H
Williams, Kenneth H

Publication Date

2025-02-28

DOI

10.1029/2024gl112927

AGU ADVANCING EARTH AND SPACE SCIENCES

Geophysical Research Letters®

RESEARCH LETTER
10.1029/2024GL112927

Key Points:
- Simulated streamflow accounts for snow dynamics, soil water storage, plant water use, interflow, recharge, groundwater gains, and losses
- Streamflow decline, low-flow extent and its duration during drought are extremely sensitive to active circulation depth of groundwater
- We recommend site-specific observations of bedrock properties at depth to more accurately predict drought response in mountain basins

Supporting Information:
Supporting Information may be found in the online version of this article.

Correspondence to:
R. W. H. Carroll,
rosemary.carroll@dri.edu

Citation:
Carroll, R. W. H., Manning, A. H., & Williams, K. H. (2025). The role of bedrock circulation depth and porosity in mountain streamflow response to prolonged drought. *Geophysical Research Letters*, *52*, e2024GL112927. https://doi.org/10.1029/2024GL112927

Received 28 OCT 2024
Accepted 7 FEB 2025

Author Contributions:
Conceptualization: Rosemary W. H. Carroll, Andrew H. Manning, Kenneth H. Williams
Data curation: Rosemary W. H. Carroll
Formal analysis: Rosemary W. H. Carroll
Funding acquisition: Kenneth H. Williams
Investigation: Rosemary W. H. Carroll, Andrew H. Manning
Methodology: Rosemary W. H. Carroll, Andrew H. Manning
Resources: Kenneth H. Williams
Visualization: Rosemary W. H. Carroll, Andrew H. Manning, Kenneth H. Williams

The Role of Bedrock Circulation Depth and Porosity in Mountain Streamflow Response to Prolonged Drought

Rosemary W. H. Carroll[1], **Andrew H. Manning**[2], **and Kenneth H. Williams**[3,4]

[1]Desert Research Institute, Reno, NV, USA, [2]United States Geological Survey, Denver, CO, USA, [3]Lawrence Berkeley National Laboratory, Berkeley, CA, USA, [4]Rocky Mountain Biological Laboratory, Gothic, CO, USA

Abstract Quantitative understanding is lacking on how the depth of active groundwater circulation in bedrock affects mountain streamflow response to a multi-year drought. We use an integrated hydrological model to explore the sensitivity of a variety of streamflow metrics to bedrock circulation depth and porosity under a plausible extreme drought scenario lasting up to 5 years. Endmember depth versus hydraulic conductivity relationships and porosity values for fractured crystalline rock are simulated. With drought, a deeper circulation system with higher drainable porosity more effectively buffers minimum flow and significantly limits perennial stream loss in comparison to a shallow circulation system. Streamflow buffering is accomplished through extensive groundwater storage loss. However, deeper circulation systems experience prolonged recovery from drought in comparison to storage-limited shallow systems. Research highlights the importance of characterizing the deeper bedrock hydrogeology in mountainous watersheds to better understand and predict drought impacts on stream ecosystem health and water resource sustainability.

Plain Language Summary Our study uses a computer model to explore how mountain streamflow responds to depth of groundwater flow in snow-fed areas. We compare streamflow in bedrock systems where groundwater flow stays close to the surface, with those where groundwater can travel hundreds of meters below ground. Our detailed model simulations account for snow accumulation and melt, soil moisture, vegetation water use and changes in water table elevations. Results indicate that shallow systems, which rapidly transport water from snowmelt and rain into streams, drain their groundwater more quickly during dry periods, with the stream going dry for months during an extreme drought. In contrast, deeper groundwater flow systems can store more water underground and release it over time to help maintain winter streamflow and sustain streamflow during dry spells. These deeper systems are better at handling prolonged droughts but take longer to recover once the drought is over. Understanding these differences helps us better predict how changes in climate will affect water supplies and ecological health in mountainous regions. More detailed studies and data are needed, particularly from the deeper bedrock flow system, to improve our models and our ability to quantify and manage water originating from mountain basins.

1. Introduction

The importance of groundwater in supporting mountain streamflow is becoming increasingly recognized. Studies indicate that groundwater comprises 10%–87% of the annual stream water budget for mountain streams (Table 1 in Somers and McKenzie (2020)), and is critical for supporting perennial streamflow and cold-water refugia for sensitive species (Kaandorp et al., 2019; Mejia et al., 2023). Though the importance of groundwater flow through the top 10 m of highly weathered saprolite is well established (Brooks et al., 2015), the importance of groundwater flow at greater depths is often uncertain and may vary considerably across different geologic settings (Markovich et al., 2019). There is growing evidence that hydrologically active groundwater commonly occurs to depths of hundreds of meters in mountain bedrock (Condon et al., 2020; Frisbee et al., 2017; Saar & Manga, 2004; Welch & Allen, 2014), though few studies have confidently constrained the active circulation depth (Manning et al., 2021). Recent modeling studies have demonstrated that seasonal and event-scale streamflow variations are sensitive to the vertical distribution of hydraulic conductivity within the active bedrock flow system (Rapp et al., 2020; Roques et al., 2022). Previous research also suggests that hydrologic response is less sensitive to interannual climate variability and more resilient to drought if water inputs exceed storage capacity (Hahm et al., 2019). However, a quantitative understanding of how mountain streamflow responds to and recovers from a multi-year drought as a function of the groundwater active circulation depth and bedrock porosity (drainable storage) is lacking. Such an understanding is needed because collecting hydrogeologic data at depth is logistically

Writing – original draft: Rosemary W. H. Carroll
Writing – review & editing: Andrew H. Manning, Kenneth H. Williams

challenging and costly. Resources to parameterize the deeper bedrock system are justified if its misrepresentation produces substantial errors in predicted mountain streamflow.

To address the potential importance of deeper groundwater, we ask, *how does the depth of groundwater flow affect streamflow during and after drought?* Effectively answering this question requires accounting for hydrologic feedbacks at fine spatial (e.g. 100–250 m) and temporal scales (≤daily) in order to estimate water and energy budgets in highly seasonal and steep landscapes. In particular, snow accumulation and melt (Baba et al., 2019; Bales et al., 2006; Mott et al., 2018) and evapotranspiration (ET) (Foster et al., 2020) are scale-dependent. Mountain hydrology is highly reliant on the lateral transport of shallow subsurface water from energy-limited, higher elevations toward downgradient convergent zones to subsidize vegetation water use (Sprenger et al., 2022), groundwater recharge below the rooting zone (Carroll et al., 2019), and streamflow generation (Li et al., 2017; Sprenger et al., 2024). Recharge supports variably saturated groundwater flow with alluvial and bedrock properties dictating highly heterogenous distributions in water table elevations and groundwater flow paths. To capture this hydrologic complexity in mountain systems and explore streamflow sensitivity to groundwater flow depth, we leverage a previously published integrated hydrological model of Copper Creek (24 km^2) (Carroll et al., 2019), a typical alpine snowmelt-dominated catchment of the Colorado River.

2. Methods

2.1. Modeling Approach

Copper Creek elevations range from 2,880 to 4,124 m (Figure S1 in Supporting Information S1). Land cover is predominantly barren rock or sparsely vegetated with conifer forests and smaller proportions of alpine meadow, shrubs and aspen (Landfire, 2015) (Figure S2a in Supporting Information S1). Snow accumulation is greatest in high-elevation cirque valleys on north-northeast aspects (Figure S4 in Supporting Information S1). The integrated hydrological model uses the U.S. Geological Survey (USGS) numerical code Groundwater and Surface water Flow (GSFLOW v2.0.0, Markstrom et al., 2008) at a 100-m grid resolution. GSFLOW dynamically couples the USGS Precipitation-Runoff Modeling System (PRMS, Markstrom et al., 2015) and the Newton formulation of the USGS 3-D Modular Groundwater Flow model (Niswonger et al., 2011) and 1-D simplification of Richards equation for the unsaturated zone (Niswonger et al., 2006). The model describes daily surface and groundwater interactions related to ET including soil ET, canopy interception, snow sublimation, and groundwater ET. Streamflow is conceptualized as containing three sources. Surface runoff is water flowing over the land surface as either infiltration or saturation excess. Interflow is the lateral movement of water through the soil zone with the soil zone typically <1 m in thickness. Groundwater flows to streams are contributions from underlying alluvial and bedrock units. Streams can gain or lose water from/to the groundwater system. Losing conditions tend to occur in low-order, high elevation tributaries during the spring and along alluvial fans (Carroll et al., 2024). The hydrologic model estimates snow accumulation and melt, interflow, groundwater recharge, change in groundwater storage, and groundwater-surface water exchanges derived from differential gradients between groundwater and stream water elevations (Huntington & Niswonger, 2012) and deeper groundwater flow as functions of subsurface hydraulic properties related to transmissivity and storage.

The land surface and soil parameterization from the original model are maintained in this study to reflect reasonable estimates in snow accumulation and melt, ET, recharge (Figure 1a) and interflow across complex, mountainous terrain. A description of the original Copper Creek model and its appropriateness for use in a sensitivity analysis of streamflow to bedrock parameterization is provided in Text S1–S2, Figure S1–S10 in Supporting Information S1. The groundwater model contains 12 layers and extends 400 m into the subsurface (Figure 1b). We assume an exponentially decaying K with depth, assuming $K = K_o e^{-A_o Z}$, where K = hydraulic conductivity at depth below land surface Z, K_o = hydraulic conductivity at land surface, and A_o = the decay coefficient (Jiang et al., 2009). The K value in the top 8 m of 10^{-5} m/s is consistent with heavily weathered saprolite (Welch & Allen, 2014). Below the saprolite, we adopt the following two A_o values to roughly mimic low and high ends of the K-range reported in literature for fractured crystalline rock (Figure 1c; Table S1 in Supporting Information S1): (a) $A_o = 0.164\ m^{-1}$, represents a shallow circulation case (henceforth "shallow case"); and (b) $A_o = 0.023\ m^{-1}$, represents a deep circulation case (henceforth "deep case") (Gleeson et al., 2011; Ranjram et al., 2015; Shmonov et al., 2003; Stober & Bucher, 2007; Welch & Allen, 2014). For shallow and deep cases, K values $\geq 10^{-7}$ m/s, which are generally associated with active flow (Welch & Allen, 2014), extend to

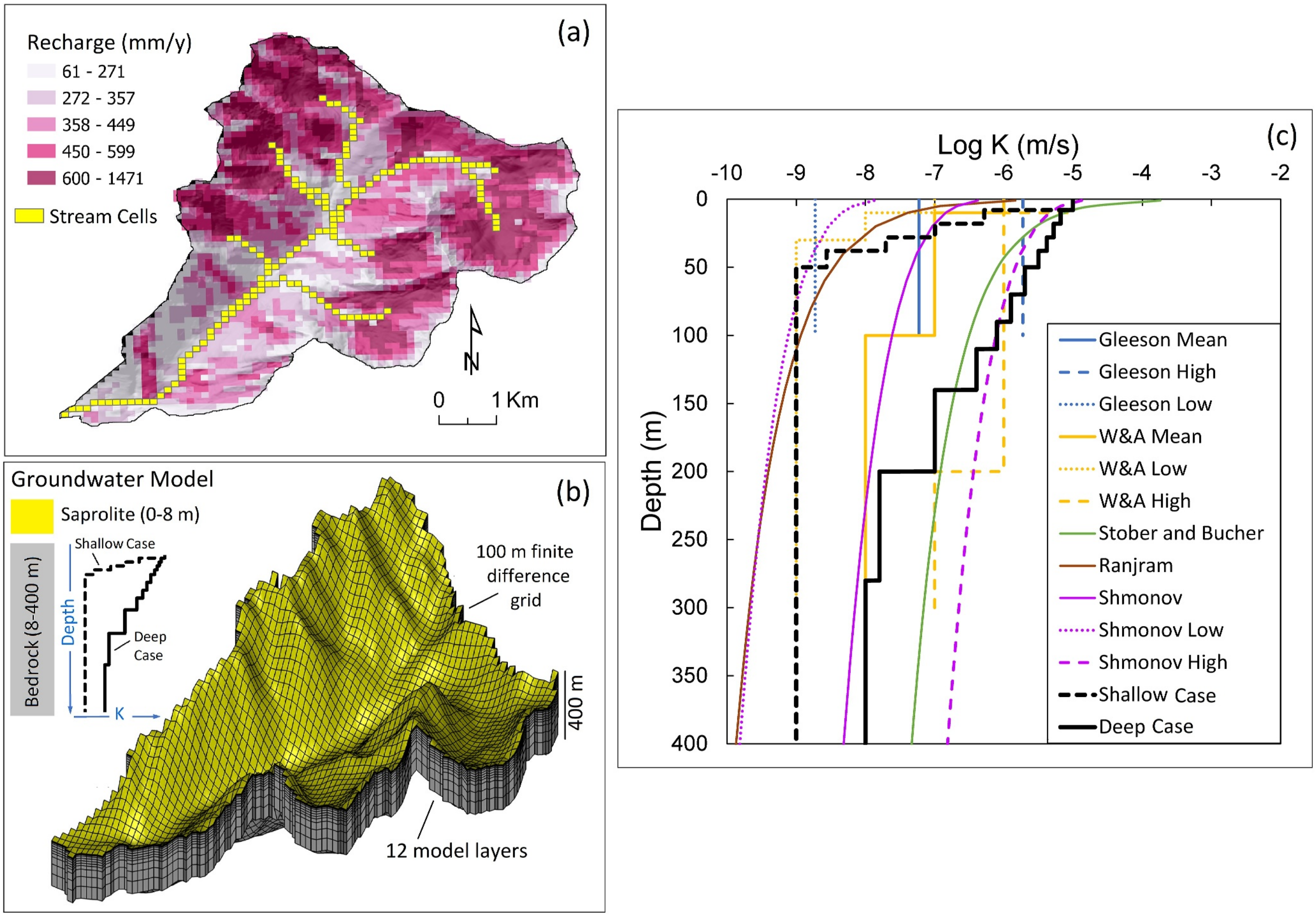

Figure 1. Integrated modeling was used to simulate hydrologic feedbacks in Copper Creek, Colorado (24 km^2). (a) The spatial distribution of simulated groundwater recharge given average climate conditions. Recharge below the rooting zone is estimated at 100 m grid resolution as functions of snow dynamics, evapotranspiration, soil moisture and interflow. Modeled stream cells are indicated. Daily recharge supports groundwater generation and is dynamically coupled to a (b) three-dimensional groundwater flow model that contains 12 layers and extends 400 m below ground surface with the bedrock (depth 8–400 m) parameterized with depth-dependent hydraulic conductivity. (c) Hydraulic conductivity (K) versus depth for modeled shallow and deep cases are compared to published relationships for fractured crystalline rock. References are provided in the text. The original model development is explained in Text S1, Figures S1–S9 in Supporting Information S1.

depths of 28 and 200 m, respectively. A minimum K of 10^{-9} m/s was assumed, given that further reductions in K yield negligible changes in groundwater flow. Reasonable low- and high-end drainable porosity values for fractured crystalline rock of 1% and 3% were assumed based on literature, along with a porosity of 4% for the saprolite (Aquilina et al., 2004; Manning et al., 2013; Mazurek et al., 2003; Stober & Bucher, 2007; Tullborg & Larson, 2006).

Each bedrock configuration was "spun-up" with daily climate conditions for an average water year (WY, defined as 1 October to 30 September) with average water year daily climate repeated until unsaturated and saturated groundwater storage stabilized. The depth of active groundwater flow and ages are calculated with particle tracking (Pollock, 2016) through the saturated portion of the groundwater model based on spatially distributed recharge fluxes extracted from GSFLOW. Particles are draped onto the water table surface and run forward in time with individual flow paths weighted by spatially explicit recharge estimates following Gusyev et al. (2014).

2.2. Climate Scenarios

Daily climate inputs rely on two snow telemetry (SNOTEL) stations that reside near the catchment (refer to Figure S1 in Supporting Information S1), Schofield (ID: 737) and Butte (ID: 380) at elevations 3,261 and 3,097 m, respectively. Minimum and maximum temperature are spatially distributed assuming a daily lapse rate between the stations and adjusted for aspect. Schofield precipitation was spatially distributed as rain using the monthly 30-

10.1029/2024GL112927

year Parameter-elevation Regressions on Independent Slopes Model (OSU, 2012) while snowfall distribution was informed by observed airborne lidar to implicitly account for snow redistribution by wind and avalanche (Painter et al., 2016) (Figures S3 and S4 in Supporting Information S1). Observed SNOTEL data for WY 1987 to 2022 were used to define climate scenarios. WY 2003 represents the closest mean condition for annual minimum and maximum daily temperature and total precipitation for the period of record (Figure S11 in Supporting Information S1). For drought conditions, daily climate inputs were stitched together based on observed hottest and driest seasonal condition at each SNOTEL location (Tables S2 and S3 in Supporting Information S1). Seasonal conditions are defined for autumn (Sept-Nov), winter (Dec-Feb), spring (Mar-May), and summer (Jun-Aug). Given all climate inputs have been observed, albeit not all together in the same water year, the concept was to generate a plausible extreme drought scenario for Copper Creek. Schofield SNOTEL seasonal conditions are provided in Figures 2a–2c. Annually, temperatures during the drought are approximately +2°C higher than the representative average water year, with the largest seasonal increases occurring in the autumn and the smallest seasonal increases occurring in the summer. SNOTEL annual precipitation during the drought is 58% reduced compared to average conditions, with the largest decreases in precipitation occurring in the spring.

2.3. Hydrologic Assessment

Streamflow metrics evaluated include average annual streamflow, shifts in perennial to non-perennial stream reaches and no flow duration, net groundwater inflow, and time to recovery. Each of these streamflow metrics were evaluated given average climate conditions and for a drought lasting up to five consecutive years. A maximum of a 5-year drought is based on the historical monthly Palmer Drought Severity Index (PDSI) for the Upper Colorado River Basin from 1895 to 2024 with the longest continuous period of PDSI > 0 values equal to 5.5 years (Figure S12 in Supporting Information S1). Model simulations extend for a total of 11 years to allow for streamflow recovery following the drought with average climate conditions simulated.

3. Results

Under average steady state recharge conditions for the shallow case, approximately 70% of groundwater flow occurs within the saprolite. Flow paths are hyper-localized with only 4% of groundwater moving at depths greater than 30 m. For the deep case, the median depth of groundwater flow is 100 m with approximately 13% of groundwater flow occurring within the saprolite and only 7% at depths >200 m. We thus consider the active circulation depth for shallow and deep cases to be 30 and 200 m, respectively, given the relatively small amount of flow occurring at greater depths (Figure S13a in Supporting Information S1). Longer and older flow originates from cirque valleys and ridge tops (Figures S13 and S14 in Supporting Information S1).

3.1. Hydrologic Effects of Drought

For average climate conditions, snow water equivalent (SWE) peaks in early April and is gone by late July (Figure 2d). Soil moisture in the winter is supported by summer/fall rain and remains stable. Soil moisture peaks in the spring in response to snowmelt (i.e., decreasing SWE) and is at a minimum in the summer due to ET (Figure S15 in Supporting Information S1). Snowmelt and increased soil moisture support recharge (Figure 2f) and interflow to streams. Streamflow increases above winter baseflow during snowmelt to peak at the end of May. As snowmelt diminishes, streamflow recedes toward baseflow with small transient increases in response to rain (Figures 2g and 2j). Baseflow is achieved in the fall as temperatures cool and vegetation senesces. Given average climate conditions, stream hydrographs for the deep and shallow cases look similar, though the shallow case tends to have slightly larger spring and summer discharge and lower winter baseflow. A 2% difference in drainable porosity has only a small effect on daily streamflow. For the deep case, stream flow source is primarily from interflow (65%) with substantial groundwater contributions (35%) and only minimal surface runoff (<1%). Stream water source for the shallow case is similar. It contains 71% interflow and 29% groundwater. For both cases, the entire river network is activated during snowmelt from mid-May to mid-June with no dry reaches simulated (non-perennial fraction = 0) (Figures 2h and 2k). Otherwise, the shallow case has a lower average fraction of the stream network going dry than the deep case due to a shallower water table depths and a greater fraction of groundwater intercepting land surface even at higher elevations.

During drought, snow accumulation is drastically reduced by 83% compared to the average climate condition, and average daily snow-covered area (SCA) declines 46% (Figure S17 in Supporting Information S1). Rising

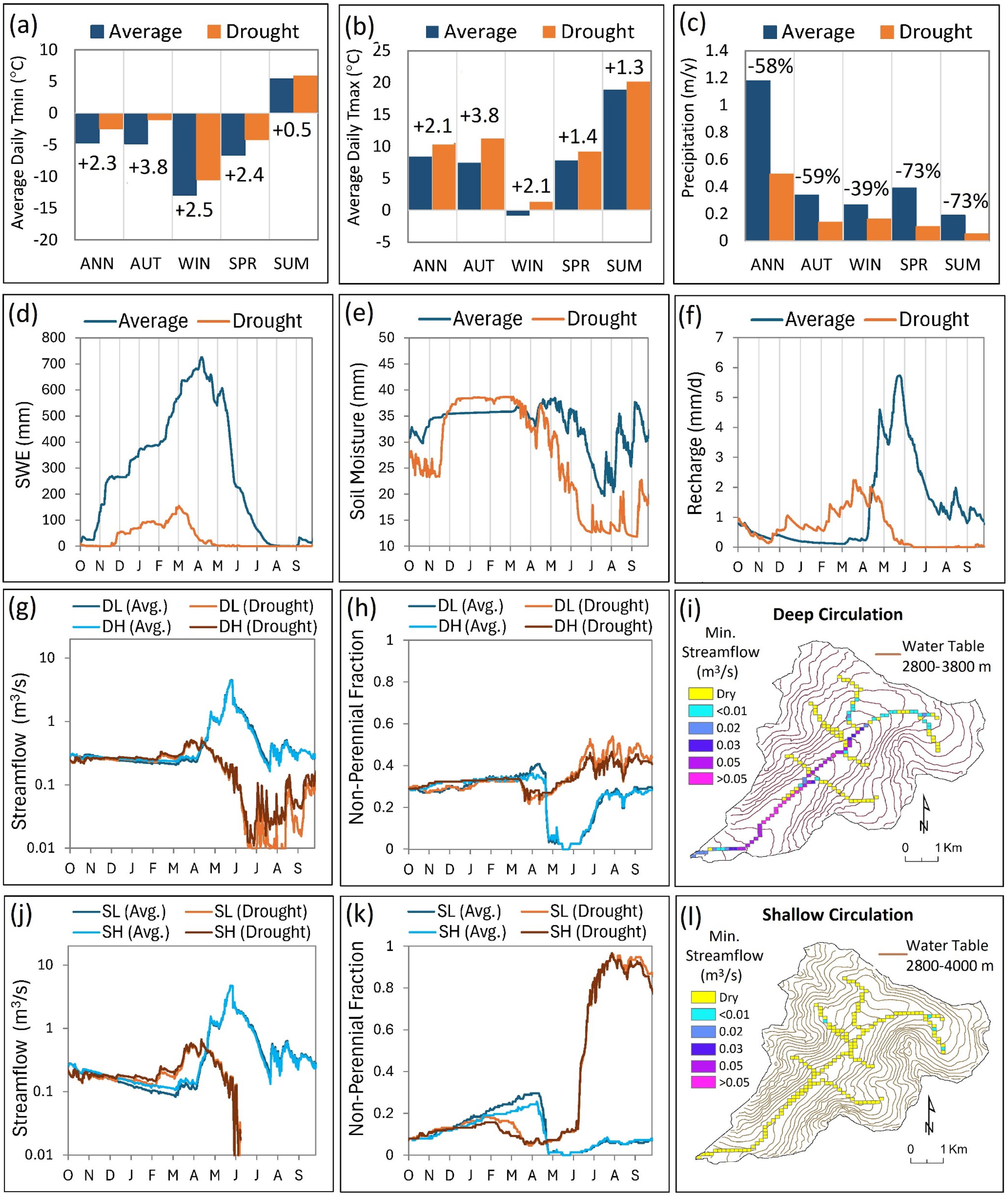
(a)
Average
Drought
Average Daily Tmin (°C)
+2.3
+3.8
+2.5
+2.4
+0.5
ANN AUT WIN SPR SUM
(b)
Average Daily Tmax (°C)
+2.1
+3.8
+2.1
+1.4
+1.3
(c)
Precipitation (m/y)
-58%
-59%
-39%
-73%
-73%
(d)
SWE (mm)
(e)
Soil Moisture (mm)
(f)
Recharge (mm/d)
(g)
DL (Avg.)
DL (Drought)
DH (Avg.)
DH (Drought)
Streamflow (m³/s)
(h)
Non-Perennial Fraction
(i)
Deep Circulation
Min. Streamflow (m³/s)
Dry
<0.01
0.02
0.03
0.05
>0.05
Water Table 2800-3800 m
1 Km
(j)
SL (Avg.)
SL (Drought)
SH (Avg.)
SH (Drought)
(k)
(l)
Shallow Circulation
Water Table 2800-4000 m

Figure 2.

10.1029/2024GL112927

temperatures increase atmospheric demand, and reduced SCA lengthens the growing season with ET increasing earlier in the year but with reduced precipitation results in an average annual decline in total ET by 22%. Despite a reduction in ET volume with drought, the ratio of ET to precipitation increases from 45% for average climate conditions to 86% under drought. Warmer temperatures result in an earlier onset of snowmelt to initially increase soil moisture, recharge and interflow contributing to streamflow. However, early water fluxes occur at the expense of all three later in the water year to result in an annual net decline. There is a 22% decline in soil moisture, 53% decline in recharge, and in year 1 of a drought, an 83% decline in interflow to streams. Low soil moisture during drought extends into the subsequent water year to reduce interflow to streams by 7% and recharge by 11% despite the return to average climate conditions.

The bulk of streamflow response to extended drought occurs within the first 2 years for all simulated cases and generally plateaus for droughts of longer duration. Average streamflow during drought drops dramatically for both deep and shallow cases (Figure 3a). However, in relative terms, average annual streamflow remains substantially higher for the deep case, being approximately 80% and 60% greater than the shallow case in year two of the drought for porosities of 3% and 1%, respectively. Perhaps more importantly, in the shallow case, the majority of the stream network goes dry in July after only 1 year of extreme drought (Figures 2j–2l and 3b) and remains dry for an extended period (approx. 3.3 months). With 2 years of drought, Copper Creek remains dry for 5.5 months (Figure S18 in Supporting Information S1). In contrast, the deep case limits non-perennial expansion and maintains streamflow exiting the catchment valley for all drought durations tested (Figures 2g–2i and 3b). Increasing drainable porosity from 1% to 3% has little effect for most streamflow metrics given a 1-year drought, but for droughts lasting two or more years, the effect is to buffer the negative effects of drought. For example, in the deep case after 2 years of drought, a 3% porosity results in 30% more streamflow, and decreases the maximum fraction on non-perennial streams up to 13% compared to the 1% porosity example. Average groundwater flow into stream channels for the shallow case given no drought is 0.15 m^3/s, or about 20% lower than the deeper case (Figure 3c). After 2 years of drought, groundwater flow in the shallow case and assuming 3% porosity is reduced by 78%. This is compared to the deeper case that experiences a 42% groundwater inflow reduction. The deeper case, however, does experience a more consistent decay in groundwater inflow with drought duration compared to the shallow case, such that after 5 years of drought, groundwater inflow to streams is diminished by 67%.

3.2. Time to Recover

The time to recovery was evaluated for average streamflow (Figure S19 in Supporting Information S1), the average fraction of stream network that is non-perennial (Figure S20 in Supporting Information S1), no-flow duration (Figure S21 in Supporting Information S1), average groundwater to streams (Figure 3e and Figure S22 in Supporting Information S1) and groundwater storage (Figure 3d and Figure S23 in Supporting Information S1). Recovery is assumed once pre-drought conditions are achieved. For groundwater flow to streams, recovery is assumed when groundwater flow is less than 0.015 m^3/s from pre-drought conditions (∼10% average condition). This was done because the exact timing of recovery is slightly uncertain in the deeper case due to the oscillation of recovery response at/near historical condition related to lag effects of recharge through its relatively thick unsaturated zone compared to the shallow case (Figure S24 in Supporting Information S1). For the shallow case given 1% porosity, streamflow metrics and groundwater storage recovered to pre-drought conditions in approximately 2 years. Increasing porosity to 3% in the shallow case increased groundwater recovery by approximately half a year for droughts lasting at least 4 years. Short recovery times in the shallow case reflect storage-limited conditions in which active groundwater storage is less than average annual recharge. Recovery time for stream metrics given a 1-year drought in the deep case and 1% porosity are approximately 3 years, with recovery of groundwater sourcing to streams increasing to 5 years with increased drought duration. For the deep case and 3% porosity, recovery time for groundwater flow to streams increases by 1 year over the 1% porosity

Figure 2. Simulated hydrologic effects given 1 year of an extreme drought in comparison to average climate conditions. Annual and seasonal climate differences at the Schofield SNOTEL: (a) average daily minimum temperature, (b) average daily maximum temperature, (c) total precipitation, with temperature (°C) and precipitation (%) differences between average and drought provided. Daily land surface responses: (d) snow water equivalent, SWE, (e) soil moisture, and (f) recharge. Hydrologic responses in the deep case: (g) daily streamflow, (h) daily fraction stream network that goes dry, or is non-perennial, and (i) 7-day minimum flow during drought for 3% porosity. Hydrologic responses for the shallow case: (j) daily streamflow, (k) daily fraction stream network that goes dry or is non-perennial, and (l) 7-day minimum flow during drought with 3% porosity. Water table contours at 50 m provided for 1 August. DL = deep case and 1% porosity, SL = shallow case and 1% porosity, DH = deep case and 3% porosity, SH = shallow case and 3% porosity.

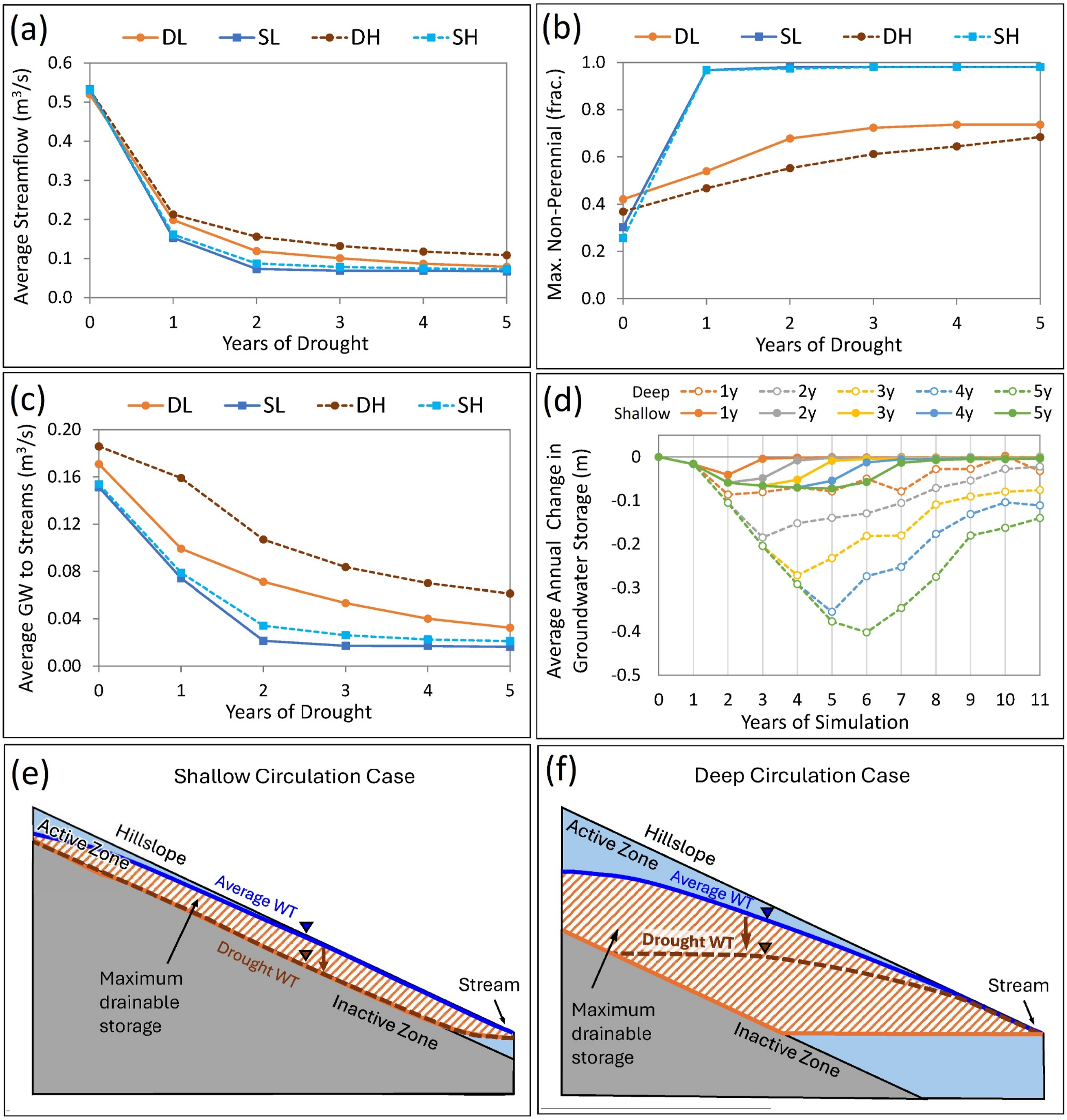

Figure 3. Hydrologic response to drought duration of 0–5 years for different bedrock parameterizations: average annual (a) streamflow, (b) maximum fraction of stream network that is dry, and (c) net groundwater to streams. (d) A comparison of groundwater storage change from average climate conditions for the deep case with 3% porosity and shallow case with 1% porosity for 1-year to 5-year drought durations followed by average climate conditions for change in groundwater storage. Diagrams schematically illustrate changing water table elevations during simulated drought and maximum drainable storage in the (e) shallow case and (f) deep case. DL = deep case, 1% porosity, SL = shallow case, 1% porosity, DH = deep case, 3% porosity, SH = shallow case, 3% porosity.

across different drought scenarios. Longer recovery in the deeper case reflects large decreases in groundwater storage during drought compared to the shallow case with recovery in the subsurface lasting up to a decade for drought durations of 3 years (Figure S25 in Supporting Information S1).

10.1029/2024GL112927

4. Discussion

Links between mountain streamflow and the depth of hydrologically active groundwater flow have been explored empirically using temperature (Briggs et al., 2018), solute concentrations (Frisbee et al., 2017) and age tracers (Carroll, Gochis, & Williams, 2020; Carroll, Manning, et al., 2020; Thiros et al., 2024); as well as numerical modeling studies given theoretical (Gleeson & Manning, 2008; Rapp et al., 2020) and real-world examples (Ameli et al., 2018; Tague et al., 2008). In particular, Rapp et al. (2020) found that stream discharge was most sensitive to shallow subsurface conductivity. We expand upon earlier models by including multi-year drought scenarios and accounting for dynamically coupled land surface and subsurface processes at high spatial and temporal resolution. Additionally, our bedrock hydraulic conductivity and porosity parameterizations span nearly the full range of values observed for crystalline rock in previous studies, to represent bedrock systems with substantially different circulation depths. For the shallow case, the majority of groundwater flow occurs in the shallow saprolite (depth <8 m), while the deep case promotes a median groundwater flow depth of 100 m.

Simulations of long-term average climate indicate similar hydrographs and stream sourcing for the shallow and deep case. Seasonally, the shallow case supports slightly higher spring and summer flow because more snowmelt and rain are transported toward streams as interflow given shallow water tables exfiltrate groundwater into the soil zone (Figure S26 in Supporting Information S1). However, steep hydraulic gradients and limited bedrock storage capacity drain groundwater more quickly and exiting streamflow out of the catchment exhibits a decreasing trend over the winter period. Higher ratios of winter streamflow to annual streamflow, or winter flow index (WFI), that are simulated for the deeper case compared to the shallower case agrees with previous research indicating larger WFI in higher permeability and porosity systems (Paznekas & Hayashi, 2016). Likewise, activation of deeper storage has been shown to increase minimum flows and potentially reduce peak flows (Bennett et al., 2023). Nonetheless, differences in hydrographs under long-term average climate conditions are not drastically different as a function of groundwater circulation depth.

During drought, streamflow is decreased, in part, through reductions in interflow related to preferential partitioning of soil water toward ET due to low snow accumulation, a longer growing season (Milly & Dunne, 2020) and lack of monsoon rain (Carroll, Gochis and Williams, 2020). Reduction in soil moisture reduces groundwater recharge. Dry soils in the fall extend through the winter and require more snowmelt in the spring to achieve the water capacity threshold necessary for initiating interflow (McNamara et al., 2005) and recharge (Carroll et al., 2024) in the year following drought. Thin mountain soils, however, lessen the cumulative influence of soil moisture on these fluxes for droughts greater than 2 years (Figure S27 in Supporting Information S1). Given land surface parameterization during drought is identical for all model scenarios, changes in soil moisture, interflow, ET and recharge are relatively the same between the deep and shallow cases.

Differences in drought response between the deep and shallow bedrock cases occur with low-flow stream metrics. Low flow is important to habitat availability, species composition, water quality, nutrient cycling and overall biodiversity (Rolls et al., 2012). For the shallow case, active groundwater storage is effectively drained in 2 years (Figure 3e) and streamflow metrics do not appreciably further decline for droughts longer than 2 years. With a 2-year drought (or greater), groundwater flow to the stream is effectively eliminated and the stream network goes dry for nearly half of the year. While theoretical, model results suggest greater ecological hardship in shallow circulation systems as drought severity increases even if drought duration is relatively short. Specifically, drought-induced declines in flow magnitude and increased duration of these events will likely reduce macroinvertebrate abundance and composition through reduced stream depth, velocity, and dissolved oxygen (Munasinghe et al., 2021); stress critical fish populations (Hakala & Hartman, 2004); and potentially increase colonization and biomass of periphyton (Suren et al., 2003). Likewise, habitat fragmentation and lost refugia during drought-induced drying of stream segments are expected to reduce species survival and recovery (Vander Vorste et al., 2020). Despite sensitivity of low-flow stream metrics to relatively short drought durations in shallow bedrock systems, resilience is also high. A return to average climate, in which recharge exceeds drainable storage, rebounds streamflow metrics to pre-drought conditions in approximately 2 years.

Tague et al. (2008), using hydrographic analysis and physically based models, attributed mediated streamflow loss during warming to deep groundwater. We also find that deeper groundwater storage release subsidizes low flow in mountain streams and does so even under extreme meteorological stress. As an example, the release of groundwater from a larger subsurface storage reservoir maintains perennial streamflow in at least 26% of its stream network even after a 5-year drought. While porosity is less influential on overall storage capacity of shallow bedrock systems, a small 2% increase in porosity in the deeper case substantially increases buffering capacity of groundwater to streams and limits non-perennial expansion. Results indicate groundwater storage declines are linear for each successive year of drought (Figure 3d). This suggests groundwater decline does not reach the maximum drainable storage available (Figure 3f) and further groundwater release could maintain perennial conditions in the catchment for longer lasting droughts. However, this buffering of streamflow is done at a cost. For example, large and persistent water table declines may degrade water quality through increased sulfate and metals concentrations (Manning et al., 2013), enhanced weathering along longer flow paths (Bondu et al., 2016), and stream waters becoming more dependent on solute-rich groundwater. In addition, for bedrock systems with deep circulation, even in a cold and wet mountain basin such as Copper Creek with ample estimated recharge under average climate conditions, the time for stream recovery is twice as long as the shallow case, and groundwater storage recovery approaches a decade following drought. Long memory in the deeper groundwater system reduces stream generation up to 5 years after the meteorological drought has ceased and makes the catchment more vulnerable to future droughts that may occur prior to full groundwater storage recovery. As climate in the Colorado River Basin headwaters becomes warmer and possible aridification propagates (Overpeck & Udall, 2020) deeper groundwater systems may eventually not recover (e.g., Peterson et al., 2021).

We acknowledge that direct observations (i.e., tracer tests), and surrogate tests for specific yield (i.e., pumping tests, water table observations, and packer tests) are difficult and expensive to perform in mountainous terrain. However, given the sensitivity of low-flow metrics to reasonable endmember parameterization of crystalline rock, and the importance of the magnitude, duration, and spatial extent of low-flow conditions during drought on ecologic health, downstream water availability, and possible implications on water quality, we recommend site-specific observations of bedrock properties at depth to better parameterize our hydrologic models and more accurately predict drought response in mountain basins.

5. Conclusions

Our study advances understanding of the effect of the depth of hydrologically active groundwater flow on streamflow response to drought by using a numerical model that integrates dynamic land surface and subsurface processes at high spatial and temporal resolution. The analysis reveals that shallow-circulating systems are considerably more sensitive to droughts of shorter (2-year) duration than deeper-circulating systems. Deeper circulating systems more effectively buffer low-flow stream conditions against prolonged drought through the release of groundwater from storage but do so at a cost of a more protracted recovery. These findings align with previous research but specifically highlight the sensitivity of streamflow magnitude and extent during low-flow periods to the active circulation depth and deeper bedrock porosity. Our results emphasize the importance of accurately characterizing the deeper bedrock hydraulic conductivity and porosity in mountainous regions, as these factors are crucial for predicting hydrologic responses to climate variability and long-term changes.

Data Availability Statement

The GSFLOW code version 2.0.0 and all documentation are provided by the U.S. Geological Survey at https://www.usgs.gov/software/gsflow-coupled-groundwater-and-surface-water-flow-model. Copper Creek GSFLOW model files (Carroll and Williams, 2024) are provided to the public with no restrictions.

Acknowledgments
Work was supported as part of the Watershed Function Science Focus Area funded by the US Department of Energy, Office of Science, Office of Biological and Environmental Research under Contract No. DE-AC02-05CH11231. Work was also supported by the U.S. Geological Survey's Mineral Resources Program. We would like to thank Dylan O'Ryan, Research Associate at Lawrence Berkeley National Laboratory for his help and support with data management.

References

Ameli, A. A., Gabrielli, C., Morgenstern, U., & McDonnell, J. J. (2018). Groundwater subsidy from headwaters to their parent water watershed: A combined field-modeling approach. *Water Resources Research*, *54*(7), 5110–5125. https://doi.org/10.1029/2017WR022356

Aquilina, L., De Dreuzy, J.-R., Bour, O., & Davy, P. (2004). Porosity and fluid velocities in the upper continental crust (2 to 4 km) Inferred from injection tests at the Soultz-sous-Forêts geothermal site. *Geochimica et Cosmochimica Acta*, *68*(11), 2405–2415. https://doi.org/10.1016/j.gca.2003.08.023

Baba, M. W., Gascoin, S., Kinnard, C., Marchane, A., & Hanich, L. (2019). Effect of digital elevation model resolution on the simulation of the snow cover evolution in the High Atlas. *Water Resources Research*, *55*(7), 5360–5378. https://doi.org/10.1029/2018WR023789

Bales, R. C., Molotch, N. P., Painter, T. H., Dettinger, M. D., Rice, R., & Dozier, J. (2006). Mountain hydrology of the western United States. *Water Resources Research*, *42*(8), W08432. https://doi.org/10.1029/2005WR004387

Bennett, K. E., Schwenk, J., Bachand, C., Gasarch, E., Stachelek, J., Bolton, W. R., & Rowland, J. C. (2023). Recent streamflow trends across permafrost basins of North America. *Frontiers in Water*, *5*, 1099660. https://doi.org/10.3389/frwa.2023.1099660

Bondu, R., Cloutier, V., Rosa, E., & Benzaazoua, M. (2016). A review and evaluation of the impacts of climate change on geogenic arsenic in groundwater from fractured bedrock aquifers. *Water, Air and Soil Pollution*, *227*(9), 296. https://doi.org/10.1007/s11270-016-2936-6

Briggs, M. A., Johnson, Z. C., Snyder, C. D., Hitt, N. P., Kurylyk, B. L., Lautz, L., et al. (2018). Inferring watershed hydraulics and cold-water habitat persistence using multi-year air and stream temperature signals. *Science of the Total Environment*, *636*, 1117–1127. https://doi.org/10.1016/j.scitotenv.2018.04.344

Brooks, P. D., Chorover, J., Fan, Y., Godsey, S. E., Maxwell, R. M., McNamara, J. P., & Tague, C. (2015). Hydrological partitioning in the critical zone: Recent advances and opportunities for developing transferable understanding of water cycle dynamics. *Water Resources Research*, *51*(9), 6973–6987. https://doi.org/10.1002/2015WR017039

Carroll, R., & Williams, K. (2024). Groundwater and surface water flow (GSFLOW) model files to explore bedrock circulation depth and porosity in Copper Creek, Colorado [Dataset]. *Environmental System Science Data Infrastructure for a Virtual Ecosystem (ESS-DIVE) Repository; Watershed Function SFA*. https://doi.org/10.15485/2453885

Carroll, R. W. H., Deems, J. S., Niswonger, R., Schumer, R., & Williams, K. H. (2019). The importance of interflow to groundwater recharge in a snowmelt-dominated headwater basin. *Geophysical Research Letters*, *46*(11), 5899–5908. https://doi.org/10.1029/2019GL082447

Carroll, R. W. H., Gochis, D., & Williams, K. H. (2020). Efficiency of the summer monsoon in generating streamflow within a snow-dominated headwater basin of the Colorado River. *Geophysical Research Letters*, *47*(23), e2020GL090856. https://doi.org/10.1029/2020GL090856

Carroll, R. W. H., Manning, A. H., Niswonger, R., Marchetti, D., & Williams, K. H. (2020). Baseflow age distributions and depth of active groundwater flow in a snow-dominated mountain headwater basin. *Water Resources Research*, *56*(12), 1–19. https://doi.org/10.1029/2020WR028161

Carroll, R. W. H., Niswonger, R. G., Ulrich, C., Varadharajan, C., Siirila-Woodburn, E. R., & Williams, K. H. (2024). Declining groundwater storage expected to amplify mountain streamflow reductions in a warmer world. *Nature Water*, *2*(5), 419–433. https://doi.org/10.1038/s44221-024-00239-0

Condon, L. E., Markovich, K. H., Kelleher, C. A., McDonnell, J. J., Ferguson, G., & McIntosh, J. C. (2020). Where is the bottom of a watershed? *Water Resources Research*, *56*(3), e2019WR026010. https://doi.org/10.1029/2019WR026010

Foster, L. M., Williams, K. H., & Maxwell, R. M. (2020). Resolution matters when modeling climate change in headwaters of the Colorado River. *Environmental Research Letters*, *15*(10), 104031. https://doi.org/10.1088/1748-9326/aba77f

Frisbee, M. D., Tolley, D. G., & Wilson, J. L. (2017). Field estimates of groundwater circulation depths in two mountainous watersheds in the western U.S. and the effect of deep circulation on solute concentrations in streamflow. *Water Resources Research*, *53*(4), 2693–2715. https://doi.org/10.1002/2016WR019553

Gleeson, T., & Manning, A. H. (2008). Regional groundwater flow in mountainous terrain: Three-dimensional simulations of topographic and hydrogeologic controls. *Water Resources Research*, *44*(10), W10403. https://doi.org/10.1029/2008WR006848

Gleeson, T., Smith, L., Moosdorf, N., Hartmann, J., Dürr, H. H., Manning, A. H., et al. (2011). Mapping permeability over the surface of the Earth. *Geophysical Research Letters*, *38*(2), L02401. https://doi.org/10.1029/2010GL045565

Gusyev, M. A., Abrams, D., Toews, M. W., Morgenstern, U., & Stewart, M. K. (2014). A comparison of particle-tracking and solute transport methods for simulation of tritium concentrations and groundwater transit times in river water. *Hydrology and Earth System Sciences*, *18*(8), 3109–3119. https://doi.org/10.5194/hess-18-3109-2014

Hahm, W. J., Dralle, D. N., Rempe, D. M., Bryk, A. B., Thompson, S. E., Dawson, T. E., & Dietrich, W. E. (2019). Low subsurface water storage capacity relative to annual rainfall decouples mediterranean plant productivity and water use from rainfall variability. *Geophysical Research Letters*, *46*(12), 6544–6553. https://doi.org/10.1029/2019GL083294

Hakala, J. P., & Hartman, K. J. (2004). Drought effect on stream morphology and brook trout (*Salvelinus fontinalis*) populations in forested headwater streams. *Hydrobiologia*, *515*(1–3), 203–213. https://doi.org/10.1023/B:HYDR.0000027330.12182.24

Huntington, J. L., & Niswonger, R. G. (2012). Role of surface-water and groundwater interactions on projected summertime streamflow in snow-dominated regions: An integrated modeling approach. *Water Resources Research*, *48*(11), W11524. https://doi.org/10.1029/2012WR012319

Jiang, X.-W., Wan, L., Wang, X.-S., Ge, S., & Liu, J. (2009). Effect of exponential decay in hydraulic conductivity with depth on regional groundwater flow. *Geophysical Research Letters*, *36*(24), L24402. https://doi.org/10.1029/2009GL041251

Kaandorp, V. P., Doornenbal, P. J., Kooi, H., Broers, H. P., & De Louw, P. G. B. (2019). Temperature buffering by groundwater in ecologically valuable lowland streams under current and future climate conditions. *Journal of Hydrology X*, *3*, 100031. https://doi.org/10.1016/j.hydroa.2019.100031

Landfire. (2015). *Existing vegetation type and cover layers*. U.S. Department of the Interior, Geological Survey. Retrieved from http://landfire.cr.usgs.gov/viewer/

Li, D., Wrzesien, M. L., Durand, M., Adam, J., & Lettenmaier, D. P. (2017). How much runoff originates as snow in the western United States, and how will that change in the future? *Geophysical Research Letters*, *44*(12), 6163–6172. https://doi.org/10.1002/2017GL073551

Manning, A. H., Ball, L. B., Wanty, R. B., & Williams, K. H. (2021). Direct observation of the depth of active groundwater circulation in an alpine watershed. *Water Resources Research*, *57*(2), 2020WR028548. https://doi.org/10.1029/2020WR028548

Manning, A. H., Verplanck, P. L., Caine, J. S., & Todd, A. S. (2013). Links between climate change, water-table depth, and water chemistry in a mineralized mountain watershed. *Applied Geochemistry*, *37*, 64–78. https://doi.org/10.1016/j.apgeochem.2013.07.002

Markovich, K. H., H Manning, A., E Condon, L., & McIntosh, J. C. (2019). Mountain-block recharge: A review of current understanding. *Water Resources Research*, *55*(11), 8278–8304. https://doi.org/10.1029/2019WR025676

Markstrom, S. L., Niswonger, R. G., Regan, R. S., Prudic, D. E., & Barlow, P. M. (2008). GSFLOW – Coupled ground-water and surface-water flow model based on the integration of the precipitation-runoff modeling system (PRMS) and the modular ground-water flow model (MODFLOW-2005). *U.S. Geological Survey Techniques and Methods*, *6-D1*, 240.

Markstrom, S. L., Regan, R. S., Hay, L. E., Viger, R. J., Webb, R. M. T., Payn, R. A., & LaFontaine, J. H. (2015). PRMS-IV, the precipitation-runoff modeling system, version 4, *U.S. Geological Survey Techniques and Methods, Book 6, Chapter B7* (p. 158). https://doi.org/10.3133/tm6B7

Mazurek, M., Jakob, A., & Bossart, P. (2003). Solute transport in crystalline rocks at Äspö—I: Geological basis and model calibration. *Journal of Contaminant Hydrology*, *61*(1–4), 157–174. https://doi.org/10.1016/s0169-7722(02)00137-7

McNamara, J. P., Chandler, D., Seyfried, M., & Achet, S. (2005). Soil moisture states, lateral flow, and streamflow generation in a semi-arid, snowmelt-driven catchment. *Hydrological Processes*, *19*(20), 4023–4038. https://doi.org/10.1002/hyp.5869

Mejia, F. H., Ouellet, V., Briggs, M. A., Carlson, S. M., Casas-Mulet, R., Chapman, M., et al. (2023). Closing the gap between science and management of cold-water refuges in rivers and streams. *Global Change Biology*, *29*(19), 5482–5508. https://doi.org/10.1111/gcb.16844

Milly, P. C. D., & Dunne, K. A. (2020). Colorado River flow dwindles as warming-driven loss of reflective snow energizes evaporation. *Science*, *367*(6483), 1252–1255. https://doi.org/10.1126/science.aay9187

Mott, R., Vionnet, V., & Grünewald, T. (2018). The seasonal snow cover dynamics: Review on wind-driven coupling processes. *Frontiers in Earth Science*, *6*, 197. https://doi.org/10.3389/feart.2018.00197

Munasinghe, D. S. N., Najim, M. M. M., Quadroni, S., & Musthafa, M. M. (2021). Impacts of streamflow alteration on benthic macroinvertebrates by mini-hydro diversion in Sri Lanka. *Scientific Reports*, *11*(1), 546. https://doi.org/10.1038/s41598-020-79576-5

Niswonger, R. G., Panday, S., & Ibaraki, M. (2011). MODFLOW-NWT, A Newton formulation for MODFLOW-2005. *U.S. Geological Survey Groundwater Resources Program, Techniques and Methods*, *6*(A37), 44.

Niswonger, R. G., Prudic, D. E., & Regan, S. R. (2006). Documentation of the unsaturated-zone flow (UZF1) package for modeling unsaturated flow between the land surface and the water table with MODFLOW-2005. *U.S. Geological Survey Techniques and Methods*, *71*.

OSU. (2012). *PRISM Climate Group*. Oregon State University. Retrieved from http://prism.oregonstate.edu

Overpeck, J. T., & Udall, B. (2020). Climate change and the aridification of North America. *Proceedings of the National Academy of Sciences*, *117*(22), 11856–11858. https://doi.org/10.1073/pnas.2006323117

Painter, T. H., Berisford, D. F., Boardman, J. W., Bormann, K. J., Deems, J. S., Gehrke, F., et al. (2016). The airborne snow observatory: Fusion of scanning lidar, imaging spectrometer, and physically-based modeling for mapping snow water equivalent and snow albedo. *Remote Sensing of Environment*, *184*, 139–152. https://doi.org/10.1016/j.rse.2016.06.018

Paznekas, A., & Hayashi, M. (2016). Groundwater contribution to winter streamflow in the Canadian Rockies. *Canadian Water Resources Journal / Revue Canadienne Des Ressources Hydriques*, *41*(4), 484–499. https://doi.org/10.1080/07011784.2015.1060870

Peterson, T. J., Saft, M., Peel, M. C., & John, A. (2021). Watersheds may not recover from drought. *Science*, *372*(6543), 745–749. https://doi.org/10.1126/science.abd5085

Pollock, D. W. (2016). User Guide for MODPATH Version 7—A Particle-Tracking Model for MODFLOW, *U.S. Geological Survey Open-File Report 2016–1086* (p. 35). https://doi.org/10.3133/ofr20161086

Ranjram, M., Gleeson, T., & Luijendijk, E. (2015). Is the permeability of crystalline rock in the shallow crust related to depth, lithology or tectonic setting? *Geofluids*, *15*(1–2), 106–119. https://doi.org/10.1111/gfl.12098

Rapp, G. A., Condon, L. E., & Markovich, K. H. (2020). Sensitivity of simulated mountain block hydrology to subsurface conceptualization. *Water Resources Research*, *56*(10), e2020WR027714. https://doi.org/10.1029/2020wr027714

Rolls, R. J., Leigh, C., & Sheldon, F. (2012). Mechanistic effects of low-flow hydrology on riverine ecosystems: Ecological principles and consequences of alteration. *Freshwater Science*, *31*(4), 1163–1186. https://doi.org/10.1899/12-002.1

Roques, C., Rupp, D. E., De Dreuzy, J.-R., Longuevergne, L., Jachens, E. R., Grant, G., et al. (2022). Recession discharge from compartmentalized bedrock hillslopes. *Hydrology and Earth System Sciences*, *26*(16), 4391–4405. https://doi.org/10.5194/hess-26-4391-2022

Saar, M. O., & Manga, M. (2004). Depth dependence of permeability in the Oregon Cascades inferred from hydrogeologic, thermal, seismic, and magmatic modeling constraints. *Journal of Geophysical Research*, *109*(B4), B04204. https://doi.org/10.1029/2003jb002855

Shmonov, V. M., Vitiovtova, V. M., Zharikov, A. V., & Grafchikov, A. A. (2003). Permeability of the continental crust: Implications of experimental data. *Journal of Geochemical Exploration*, *78–79*, 697–699. https://doi.org/10.1016/s0375-6742(03)00129-8

Somers, L. D., & McKenzie, J. M. (2020). A review of groundwater in high mountain environments. *Wiley Interdisciplinary Reviews: Water*, *7*(6), e1475. https://doi.org/10.1002/wat2.1475

Sprenger, M., Carroll, R. W. H., Dennedy-Frank, J., Siirila-Woodburn, E. R., Newcomer, M. E., Brown, W., et al. (2022). Variability of snow and rainfall partitioning into evapotranspiration and summer runoff across nine mountainous catchments. *Geophysical Research Letters*, *49*(13), e2022GL099324. https://doi.org/10.1029/2022GL099324

Sprenger, M., Carroll, R. W. H., Marchetti, D., Bern, C., Beria, H., Brown, W., et al. (2024). Stream water sourcing from high-elevation snowpack inferred from stable isotopes of water: A novel application of d-excess values. *Hydrology and Earth System Sciences*, *28*(7), 1711–1723. https://doi.org/10.5194/hess-28-1711-2024

Stober, I., & Bucher, K. (2007). Hydraulic properties of the crystalline basement. *Hydrogeology Journal*, *15*(2), 213–224. https://doi.org/10.1007/s10040-006-0094-4

Suren, A. M., Biggs, B. J. F., Kilroy, C., & Bergey, L. (2003). Benthic community dynamics during summer low-flows in two rivers of contrasting enrichment 1. Periphyton. *New Zealand Journal of Marine and Freshwater Research*, *37*(1), 53–70. https://doi.org/10.1080/00288330.2003.9517146

Tague, C., Grant, G., Farrell, M., Choate, J., & Jefferson, A. (2008). Deep groundwater mediates streamflow response to climate warming in the Oregon Cascades. *Climatic Change*, *86*(1–2), 189–210. https://doi.org/10.1007/s10584-007-9294-8

Thiros, N. E., Siirila-Woodburn, E. R., Sprenger, M., Williams, K. H., Dennedy-Frank, J. P., Carroll, R. W. H., & Gardner, W. P. (2024). Old-Aged groundwater contributes to mountain hillslope hydrologic dynamics. *Journal of Hydrology*, *635*, 131193. https://doi.org/10.1016/j.jhydrol.2024.131193

Tullborg, E.-L., & Larson, S. A. (2006). Porosity in crystalline rocks – A matter of scale. *Engineering Geology*, *84*(1–2), 75–83. https://doi.org/10.1016/j.enggeo.2005.12.001

Vander Vorste, R., Obedzinski, M., Nossaman Pierce, S., Carlson, S. M., & Grantham, T. E. (2020). Refuges and ecological traps: Extreme drought threatens persistence of an endangered fish in intermittent streams. *Global Change Biology*, *26*(7), 3834–3845. https://doi.org/10.1111/gcb.15116

Welch, L. A., & Allen, D. M. (2014). Hydraulic conductivity characteristics in mountains and implications for conceptualizing bedrock groundwater flow. *Hydrogeology Journal*, *22*(5), 1003–1026. https://doi.org/10.1007/s10040-014-1121-5

References From the Supporting Information

Berghuijs, W. R., Woods, R. A., & Hrachowitz, M. (2014). A precipitation shift from snow towards rain leads to a decrease in streamflow. *Nature Climate Change*, *4*(7), 583–586. https://doi.org/10.1038/nclimate2246

Budyko, M. I. (1974). *Climate and life*. Elsevier.

Carey, S. K., Tetzlaff, D., Seibert, J., Soulsby, C., Buttle, J., Laudon, H., et al. (2010). Inter-comparison of hydro-climatic regimes across northern catchments: Synchronicity, resistance and resilience. *Hydrological Processes*, *24*(24), 3591–3602. https://doi.org/10.1002/hyp.7880

Carroll, R. W. H., Bearup, L. A., Brown, W., Dong, W., Bill, M., & Willams, K. H. (2018). Factors controlling seasonal groundwater and solute flux from snow-dominated basins. *Hydrological Processes*, *32*(14), 2187–2202. https://doi.org/10.1002/hyp.13151

Carroll, R. W. H., & Williams, K. H. (2019). *Discharge data collected within the East River for the Lawrence Berkeley National Laboratory watershed function science focus area (water years 2015–2018)*. ESS-DIVE. https://doi.org/10.21952/WTR/1465929

Gaskill, D. L. (1991). *Geologic map of the gothic quadrangle, Gunnison County, Colorado*, *Geologic quadrangle*. US Geological Survey. https://doi.org/10.3133/gq1689

Jensen, M. E., Rob, D. C. N., & Franzoy, C. E. (1969). Scheduling irrigations using climate-crop-soil data. In *National Conference on Water Resources Engineering of the American Society of Civil Engineers* (p. 20).

NRCS. (1991). *Web Soil Survey*. United States Department of Agriculture. Retrieved from http://websoilsurvey.nrcs.usda.gov/

Oyler, J. W., Dobrowski, S. Z., Ballantyne, A. P., Klene, A. E., & Running, S. W. (2015). Artificial amplification of warming trends across the mountains of the western United States. *Geophysical Research Letters*, *42*(1), 153–161. https://doi.org/10.1002/2014gl062803

Sexstone, G. A., Clow, D. W., Stannard, D. I., & Fassnacht, S. R. (2016). Comparison of methods for quantifying surface sublimation over seasonally snow-covered terrain. *Hydrological Processes*, *30*(19), 3373–3389. https://doi.org/10.1002/hyp.10864

U.S. Geological Survey. (2019). National Elevation Dataset (NED). Retrieved from https://catalog.data.gov/dataset/usgs-national-elevation-dataset-ned

Voepel, H., Ruddell, B., Schumer, R., Troch, P. A., Brooks, P. D., Neal, A., et al. (2011). Quantifying the role of climate and landscape characteristics on hydrologic partitioning and vegetation response. *Water Resources Research*, *47*(8), W00J09. https://doi.org/10.1029/2010WR009944

Wang, D., & Tang, Y. (2014). A one-parameter Budyko model for water balance captures emergent behaviour in Darwinian hydrologic models. *Geophysical Research Letters*, *41*(13), 4569–4577. https://doi.org/10.1002/2014GL60509